

Full spin polarization of complex ferrimagnetic bismuth iron garnet probed by magneto-optical Faraday spectroscopy

Marwan Deb,^{*} Elena Popova, Arnaud Fouchet, and Niels Keller

GEMaC, CNRS–Université de Versailles St. Quentin en Yvelines, 45 avenue des Etats-Unis, 78035 Versailles Cedex, France

(Received 8 March 2013; published 12 June 2013)

We investigate the spin-dependent electronic density of states near and above the Fermi level in bismuth iron garnet (BIG), $\text{Bi}_3\text{Fe}_5\text{O}_{12}$, by magnetic circular dichroism and magneto-optical Faraday spectroscopy. BIG is a recently synthesized material, as its preparation requires special nonequilibrium conditions. Its scientific and applicative interest resides in huge specific Faraday rotation of the incident light, useful for magneto-optic applications. We show experimentally the presence of spin gaps in the conduction band as recently predicted theoretically by Oikawa *et al.* [T. Oikawa, S. Suzuki, and K. Nakao, *J. Phys. Soc. Jpn.* **74**, 401 (2005)]. In the range of photon energies, where full spin polarization is expected, completely asymmetric Faraday hysteresis loops were observed, similar to those observed in half-metals such as $(\text{Pr},\text{La})_{0.7}\text{Ca}_{0.3}\text{MnO}_3$ and Fe_3O_4 . These results were modeled using even and odd (with respect to magnetization) contributions into hysteresis loops. The odd contribution appears only in the energy ranges where the density of states is fully spin polarized and vanishes at the Curie temperature. These results open a new perspective for the use of bismuth iron garnet in optic spintronics at room temperature and above.

DOI: [10.1103/PhysRevB.87.224408](https://doi.org/10.1103/PhysRevB.87.224408)

PACS number(s): 73.20.At, 78.20.Ls, 75.50.Gg

Knowledge of the spin-dependent band structure is particularly important in magnetic systems with respect to their electronic properties. In a ferromagnetic system, the difference in the spin-resolved density of states $[N(E)]$ for up and down spins describes the static magnetization and is translated for a conducting system into a spin-polarized charge current at the Fermi energy level (E_F). This effect is at the basis of modern spintronics.¹ For ferromagnetic insulators this difference in spin-dependent density of states at the Fermi level is exploited, for example, for spin filtering.^{2,3} Furthermore, materials exhibiting gaps in one spin state with respect to the other are natural polarizers for photons in the corresponding energy range.

The Fermi surface in conducting systems is generally probed by de Haas–van Alphen or Shubnikov–de Haas measurements. Nevertheless, these analyses do not give access to the spin-dependent electron states. Their determination requires spin- and angular-resolved photoemission studies,⁴ spin-resolved tunneling spectroscopy,⁵ superconducting point contact spectroscopy,⁶ or giant/tunnel magnetoresistance measurements. The limitation of the two latter techniques is due to the fact that they only probe the spin-dependent $N(E_F)$ at the Fermi level. By comparison, magneto-optical (MO) spectroscopy in large spectral range represents an attractive tool to probe the spin-dependent electronic states for energies above E_F through the circular magnetic dichroism (CMD). This technique has recently been used to clarify the spin-dependent electronic structure in half-metals⁷ and complex magnetic semiconductor films.^{8,9} CMD is particularly interesting for magnetic insulators and is described commonly as Faraday ellipticity (ε_F). The amplitude of ε_F at fixed photon energy is determined by the difference in the absorption of the right-hand (RCP) and left-hand (LCP) circular polarization.⁹

This technique will be used to probe bismuth iron garnet (BIG), $\text{Bi}_3\text{Fe}_5\text{O}_{12}$, as this magnetic oxide has the highest specific magneto-optical Faraday rotation combined with a great transparency in the visible and infrared region (band

gap ~ 2.3 eV).¹⁰ Based on these exceptional properties, BIG has been used to fabricate high-performance magneto-optical photonic crystals^{11,12} and optical isolators.¹³ The microscopic origin of this strong magneto-optical effect was first attributed by Wittekoek and Lacklison¹⁴ to a large spin-orbit coupling induced by the hybridization of the Bi-6s with the O-2p and Fe-3d orbitals. Recently, this idea was supported by a first-principle study of the spin-orbit interaction in bismuth and yttrium iron garnet based on a spin-resolved fully relativistic band structure calculation performed by Oikawa *et al.*¹⁵ The resulting spin-resolved total density of states (DOS) is schematically illustrated in Fig. 1. First, it shows that BIG is a ferrimagnetic insulator exhibiting 100% spin polarization at E_F . Furthermore, the bottom of the conduction band is spin-split with a difference of 0.3 eV for spin-up and spin-down states. In this energy range, a gap in $N(E)$ for spin-down states is calculated. At higher energies, an additional gap is predicted this time for spin-up states. It starts at 0.7 eV above the bottom of the conduction band and has a width of about 0.5 eV. These two energy ranges with 100% spin polarization in the conduction band are presented by the shaded areas in Fig. 1. In these one-state spin bands, one should expect that only photons of LCP helicity should be absorbed for lower spin-density gap and of RCP helicity for the upper spin gap. As a consequence, CMD should be maximal and have opposite sign for the respective energy ranges. Furthermore, the transmitted light in both energy ranges should be completely circular polarized.

In this paper, we report an experimental confirmation of spin-dependent electronic structure in ferrimagnetic bismuth iron garnet via magneto-optical Faraday spectroscopic study in the visible and ultraviolet spectral range.

The CMD measurements have been carried out in polar Faraday configuration using a custom designed magneto-optical magnetometer based on 90° polarization-modulation technique. In this setup, the light emitted from a 100-W Hg arc lamp is polarized by a calcite Glan-Taylor prism and modulated at a frequency of 50 kHz with a Hinds photoelastic modulator

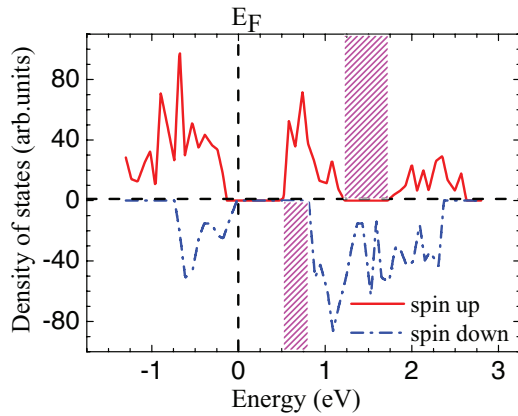


FIG. 1. (Color online) The density of states calculated for bismuth iron garnet using density functional theory (adapted from Ref. 23). The shaded areas denote the DOS with only one kind of spin state in the conduction band. The vertical dashed line indicates the Fermi level.

(PEM). After its interaction with the sample, the light passes through an analyzer before entering a monochromator. The resulting monochromatic light is transformed into an electric current by a photomultiplier detector and demodulated by two lock-in amplifiers referenced to the first and second harmonic of PEM frequency to provide a measurement of Faraday ellipticity (ε_F) and the Faraday rotation (Θ_F), respectively. For the temperature measurements, the sample is mounted in a special optical furnace allowing variation of the sample temperature from 300 to 1000 K. Note that in this work all hysteresis loops were measured in quasistatic mode and the small paramagnetic polar Faraday contribution induced by the substrate is carefully subtracted to obtain the intrinsic Faraday signal of the BIG films. The samples were grown on $\text{Gd}_3\text{Ga}_5\text{O}_{12}(001)$ (GGG) substrates by pulsed laser deposition setup and characterized *in situ* using reflection high-energy electron diffraction and ellipsometry and *ex situ* by x-ray diffraction and transmission electronic microscopy. A more detailed description of the growth conditions and an investigation of the structural and magnetic properties of the films can be found in Ref. 16.

Figure 2 shows a typical hysteresis loop of the Faraday rotation (Θ_F) versus magnetic field ($\mu_0 H$) at a wavelength

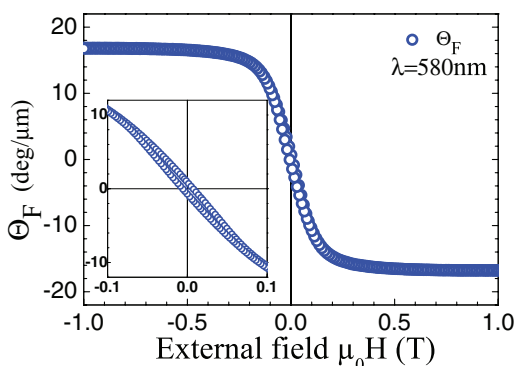


FIG. 2. (Color online) Magneto-optic hysteresis loop of the Faraday rotation measured at room temperature at a wavelength of 580 nm. The inset shows a magnified view of the region around 0 T.

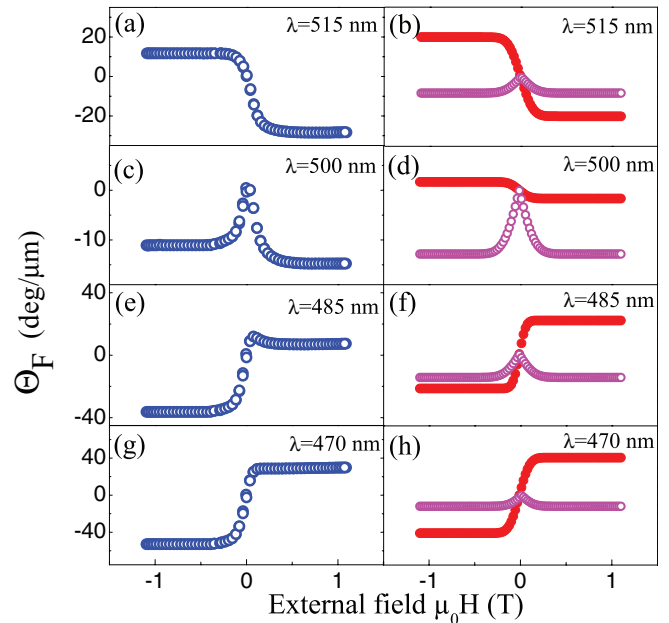


FIG. 3. (Color online) Magneto-optic hysteresis loops of the Faraday rotation measured at room temperature at different wavelengths and their deconvolution into odd and even contributions. The measurements are presented in (a), (c), (e), and (g): (a) 515 nm, (c) 500 nm, (e) 485 nm, (g) 470 nm. The odd (filled symbols) and even (open symbols) contributions to hysteresis loops are plotted separately in (b), (d), (f), and (h) for every wavelength (see text for more details).

of 580 nm. The loop has a symmetrical shape with a small coercive field of 75 Oe and very weak remanence. This weak remanence reveals that the easy magnetization axis is in the film plane. The Faraday rotation at saturation ($\Theta_{F\text{sat}}$) is about $-17 \text{ deg}/\mu\text{m}$. Typical values reported in the literature are in the range from -14 to $-19 \text{ deg}/\mu\text{m}$ at this wavelength.^{16–18} Using the same approach as employed by Vertruyen *et al.*,¹⁸ the magnetization at saturation ($\mu_0 M_S$) can be extracted from the polar hysteresis loop while neglecting the magnetocrystalline anisotropy field H_K with respect to the demagnetizing field H_d . The determined value is about $1440 \pm 40 \text{ Oe}$, in agreement with previous work.^{16,18}

Following the spectral variation of the Faraday rotation,¹⁹ a highly complex dependency of the hysteresis loop shape on the incident photon wavelength can be observed and is interpreted within the frame of crystal electrical field scheme¹⁹ or within the frame of the calculated band structure.¹⁵ As can be seen, $\Theta_F(\lambda)$ changes its sign at ~ 500 and $\sim 350 \text{ nm}$. During this sign inversion, hysteresis Faraday loops present dissymmetry as can be seen around 500 nm in Fig. 3. Although the shape of the Faraday hysteresis loop at $\lambda = 515 \text{ nm}$ [Fig. 3(a)] is similar to the one observed at 580 nm, Θ_F at saturation has a larger value for positive magnetic fields than for the negative fields. Furthermore, the Θ_F hysteresis loops are completely asymmetric at the wavelengths of 500 and 485 nm [Figs. 3(c) and 3(e)]. Finally, we see that the hysteresis loop at 470 nm has an opposite sign compared to the one at 515 nm and only a weak asymmetry. This sign inversion is in good agreement with spectroscopic study of BIG in the visible and ultraviolet range.^{19,20}

Such asymmetric hysteresis loops have already been observed for in-plane magneto-optical measurements in half-metallic Heusler alloys^{21,22} and certain half-metallic systems such as Fe_3O_4 (Ref. 23) or praseodymium-based manganites.^{24,25} For these systems, the asymmetric hysteresis loops have been decomposed into an even and an odd part, where the latter represents the standard magnetic hysteresis loop. Up to now, the largest amplitudes for the even contribution among all magnetic systems have been recorded for Heusler systems.²¹ This even contribution is also called the quadratic magneto-optical effect (QMOE) and its signal has been related to two mixed terms in magnetization, $M_L M_T$ and $M_L^2 - M_T^2$, where M_L and M_T are the longitudinal and transversal MOE, which are proportional to in-plane magnetization components.^{21,22} However, the observation of the even contribution for the out-of-plane magnetization component by Zhong *et al.*²⁶ reveals that this phenomenon is more complicated. Magneto-optical study of some manganite films [for example, $(\text{Pr,L a})_{0.7}\text{Ca}_{0.3}\text{MnO}_3$] has shown a more complex magneto-optical signal. In addition to linear magneto-optical effect, two distinct even magneto-optical contributions have been observed in this system with different temperature dependences and attributed to QMOE and the magnetorefractive effect (MRE).^{24,25} More recently, the even magneto-optical signal has been shown in magnetite Fe_3O_4 by Caicedo *et al.*²³ The temperature dependence of the even contribution shows that its amplitude is largest close to the Verwey temperature (around 100 K), and the origin of the even contribution is also attributed to the MRE. The even contributions to all these systems have been attributed to different physical origins and not understood as a single phenomenon. Nevertheless, the comparison of the electronic structure of all these magnetic systems (Heusler alloys, manganite, and magnetite) shows that they possess 100% spin polarization at the Fermi level.

To explain the observed anomalous hysteresis loops of BIG, we apply the same phenomenological analysis while decomposing them into a contribution proportional to M [i.e., odd contribution with $\Theta_F^{\text{odd}}(H) = -\Theta_F^{\text{odd}}(-H)$] and into a contribution proportional to M^2 [i.e., even contribution with $\Theta_F^{\text{even}}(H) = -\Theta_F^{\text{even}}(-H)$]. The even and odd contributions extracted from the polar hysteresis loops are displayed in Figs 2(b), 2(d), 2(f), and 2(h). We observed that the amplitude of both contributions depends on the wavelength of the incident light. Indeed, the even contribution in the polar magneto-optical signal is strong in the wavelength range where the hysteresis loop is largely distorted, whereas the odd contribution is more important for the symmetrical hysteresis loops. To further highlight this phenomenon, we show the spectral dependency of the odd and even contributions in the wavelength range from 300 to 700 nm in Fig. 4. Θ_F^{odd} changes its sign from negative to positive for wavelengths smaller than 500 nm as expected for BIG.^{19,20} On the other hand, Θ_F^{even} shows a complex spectral dependency. For a wavelength above 530 nm, no Θ_F^{even} contribution is detected. However, for wavelengths between 530 and 350 nm, Θ_F^{even} has a negative sign with two pronounced peaks. The peak around 490 nm has a maximal value of $-16 \text{ deg}/\mu\text{m}$ and occurs at the vicinity of the experimental band gap of 2.3 eV. The latter has been determined from optical absorption measurements of the sample. However, the second peak in Θ_F^{even} appears at

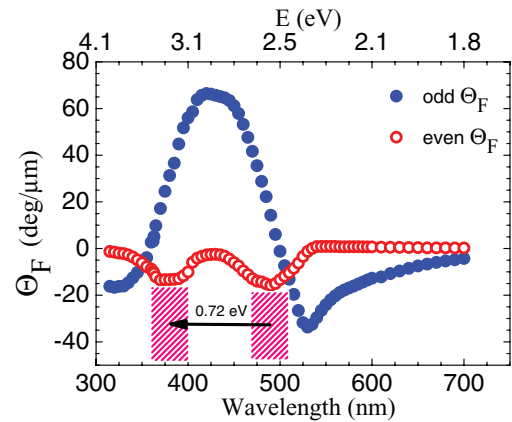


FIG. 4. (Color online) Spectral dependence of the odd (filled symbols) and even (open symbols) components of polar Faraday rotation at 300 K.

photon energies of $\sim 3.0 \text{ eV}$, i.e., 0.7 eV above the experimental band gap. These measurements have been performed on several batches of BIG samples grown on different substrates (GGG, substituted GGG, and $\text{Y}_3\text{Al}_5\text{O}_{12}$) and Θ_F^{even} is always observed. Control MO measurements were performed on epitaxial and polycrystalline yttrium iron garnet (YIG) films (not shown here) in the same wavelength range. The expected spectral dependency of $\Theta_F(\lambda)$ ^{27,28} is observed, and the Θ_F^{even} component is not detected, showing that this phenomenon is only present for bismuth iron garnet.

In order to understand this behavior in more detail, the temperature dependences of Θ_F^{odd} and Θ_F^{even} were studied. The corresponding thermal variations are shown in Fig. 5. For $\Theta_F^{\text{odd}}(T)$, we find a regular decrease with increasing temperature following the expected Brillouin behavior,²⁹ until $\Theta_F^{\text{odd}}(T)$ vanishes at the Curie temperature T_C . This behavior is similar to the one measured for thick BIG films by traditional volume magnetometry methods such as a vibrating sample magnetometer and a superconducting quantum interference device.³⁰ In contrast, $\Theta_F^{\text{even}}(T)$ decreases linearly with the temperature and vanishes also at the Curie temperature. The linear dependency is observed for several wavelengths between 365 and 500 nm and apparently is an intrinsic property of even

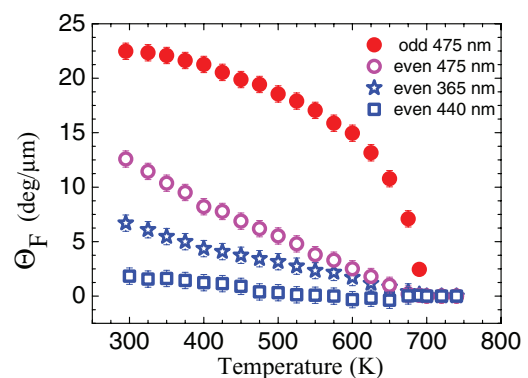


FIG. 5. (Color online) Temperature dependence of the odd (filled symbols) and even (open symbols) components of the polar Faraday rotation at different wavelengths between 365 and 500 nm. All contributions vanish at the Curie temperature.

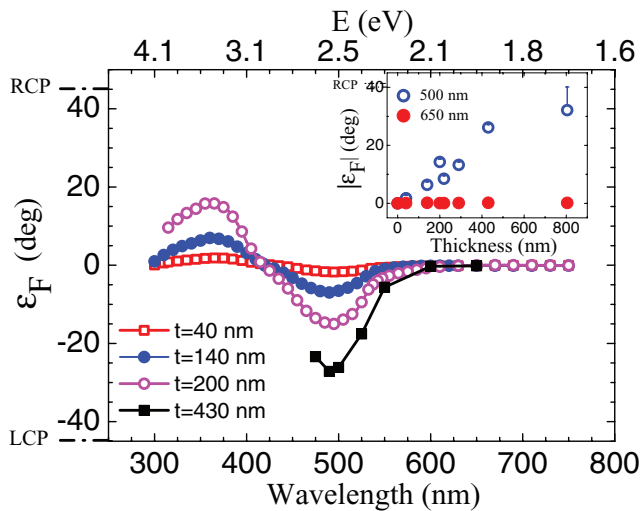


FIG. 6. (Color online) Spectral dependence of the ellipticity angle measured for several BIG films in transmission geometry. The inset shows the thickness dependence of the ellipticity angle at the wavelengths of 650 and 500 nm.

magneto-optical contribution for BIG film. In addition, the disappearance of $\Theta_F^{\text{even}}(T)$ above T_C unambiguously relates to the long-range magnetic order of the BIG film, which in its turn is related to the spin-resolved density of state at the Fermi level.

Now, we will compare our results with the theoretical $N(E)$ calculations. First, we can observe a difference in the band-gap energy determined experimentally for BIG (2.3 eV) and the calculated band gap (0.5 eV).²³ It is well known that a shortcoming of the local spin-density approximation is the underestimation of the theoretical band gap in strongly correlated systems.²³ Nevertheless, mapping $\Theta_F^{\text{even}}(E)$ of Fig. 4 onto the spin-resolved band structure of the energy above E_F (Fig. 1) shows that the two peaks of $\Theta_F^{\text{even}}(E)$ are entirely consistent with the gaps in the spin-resolved density of states in the conduction band. Both peaks have the same qualitative behavior. The first peak of $\Theta_F^{\text{even}}(E)$ starts from a photon energy of 2.3 eV (i.e., band-gap energy) and reaches its maximum at 2.56 eV. In the corresponding energy range (0.5–0.8 eV in Fig. 1), the conduction band is predicted to be fully spin polarized (spin up). In addition, the decrease in amplitude of $\Theta_F^{\text{even}}(E)$ is theoretically linked to the increase of the spin-down density of states, thus to the relative decrease in the differential state density between up and down spin. Since the same behavior characterizes the second peak in $\Theta_F^{\text{even}}(E)$, we can conclude the strong dependency between the even amplitude and the state density difference between up and down spin.

The theoretical prediction of gaps in the spin-resolved DOS implies selective absorption of photon with only one helicity (RCP or LCP). To confirm the theoretical spin-dependent

density of states, we measured the spectral dependence of the ellipticity angle of light polarization ε_F in transmission geometry. ε_F correlates to the difference in absorption between the right and left circular polarization. The amplitude of ε_F is carefully calibrated with a Soleil-Babinet compensator and its spectral dependency at room temperature is presented in Fig. 6 for four samples with different thicknesses. The ε_F spectra exhibit two sharp peaks with opposite signs and almost equal amplitude and are centered, respectively, at the vicinity of energy gap and at 0.73 eV above the band gap for all thicknesses. The change in sign of ε_F clearly demonstrates the preferential absorption of photons with opposite helicity for the two maxima and is in agreement with the inversion of the DOS between up and down spin predicted by the theoretical study illustrated in Fig. 1. This result confirms the high difference in DOS between spin-up and spin-down state in the conduction band in this energy range. On an absolute scale the presence of a gap in one of the spin-DOSs should result in ε_F values of $\pm 45^\circ$ for RCP and LCP. The inset of Fig. 6 presents the thickness dependence of ε_F . It shows a significant increase in ε_F with thickness. ε_F reaches values of 30° at 400 nm. The data point at 800-nm thickness gives a lower bound for ε_F as expected, as the sample presents an impurity phase of BiFeO₃ which absorbs both photon helicities. We extrapolate a theoretical value of $\varepsilon_F \sim 40^\circ$ at 800 nm from measurements of samples presenting also an impurity phase at thicknesses of 200 and 400 nm (not shown here). This very large value for the ellipticity angle of almost 45° reveals a nearly complete circular polarization of light after interaction with the sample. In comparison to single-crystal Fe₃O₄ and YIG, ε_F of BIG is respectively 200 and 16 times larger than the maximum values measured in the literature. In partial conclusion, the determination of the ellipticity angle as a function of wavelength and sample thickness demonstrates the presence of a huge DOS difference for spin-up and spin-down states.

Finally, in this paper, we emphasize the possibility to probe spin-electronic state for energy near and above E_F in BIG with spectroscopic Faraday measurements. Spectral Faraday rotation has shown that its complex dependency is induced by two distinct contributions into the hysteresis loops. In addition to the linear magneto-optical effect related to M , an even contribution is presented with amplitude related to the polarization of the spin state. Furthermore, the sign of the spin polarization has been determined by Faraday ellipticity. Huge polarization of DOS in two energy ranges is apparent around 2.5 and 3.5 eV with spin-polarization inversion in perfect agreement with DOS calculation in the conduction band. The work reported in this paper is important in elucidating the spin-polarization range energy of almost fully polarized BIG at room temperature and opens a new perspective for this material in optic spintronics applications.

*Corresponding author: deb@physique.uvsq.fr

¹I. Žutić, J. Fabian, and S. Das Sarma, *Rev. Mod. Phys.* **76**, 323 (2004).

²S. Matzen, J. B. Moussy, R. Mattana, K. Bouzehouane, C. Deranlot, F. Petroff, J. C. Cezar, M.-A. Arrio, P. Saintavrit, C. Gatel, B. Warot-Fonrose, and Y. Zheng, *Phys. Rev. B* **83**, 184402 (2011).

- ³Y. F. Chen and M. Ziese, *Phys. Rev. B* **76**, 014426 (2007).
- ⁴Y. Ohtsubo, S. Hatta, N. Kawai, A. Mori, Y. Takeichi, K. Yaji, H. Okuyama, and T. Aruga, *Phys. Rev. B* **86**, 165325 (2012).
- ⁵R. Wiesendanger, *Rev. Mod. Phys.* **81**, 1495 (2009).
- ⁶S. Piano, R. Grein, C. J. Mellor, K. K. Vyborny, R. Champion, M. Wang, M. Eschrig, and B. L. Gallagher, *Phys. Rev. B* **83**, 081305(R) (2011).
- ⁷S. Bordács, I. Kézsmárki, K. Ohgushi, and Y. Tokura, *New J. Phys.* **12**, 053039 (2010).
- ⁸V. Antonov, B. Harmon, and A. Yaresko, *Electronic Structure and Magneto-Optical Properties of Solids, 1st ed.* (Springer, Berlin, 2004).
- ⁹K. Ando, in *Magneto-Optics*, edited by S. Sugano and N. Kojima, Springer-Verlag Series in Solid-State Science Vol. 128 (Springer, Berlin, 2000), pp. 211–244.
- ¹⁰S. Kahl, V. Popov, and A. M. Grishin, *J. Appl. Phys.* **94**, 5688 (2003).
- ¹¹L. Magdenko, E. Popova, M. Vanwolleghem, C. Pang, F. Fortuna, T. Maroutian, P. Beauvillain, N. Keller, and B. Dagens, *Microelectron. Eng.* **87**, 2437 (2010).
- ¹²A.M. Grishin, S. I. Khartsev, and H. Kawasaki, *Appl. Phys. Lett.* **90**, 191113 (2007).
- ¹³T. Hibiya, T. Ishikawa, and Y. Ohta, *IEEE Trans. Magn.* **22**, 11 (1986).
- ¹⁴S. Wittekoek and D. E. Lacklison, *Phys. Rev. Lett.* **28**, 740 (1972).
- ¹⁵T. Oikawa, S. Suzuki, and K. Nakao, *J. Phys. Soc. Jpn.* **74**, 401 (2005).
- ¹⁶E. Popova, L. Magdenko, H. Niedoba, M. Deb, B. Dagens, B. Berini, M. Vanwolleghem, C. Vilar, F. Gendron, A. Fouchet, J. Scola, Y. Dumont, M. Guyot, and N. Keller, *J. Appl. Phys.* **112**, 093910 (2012).
- ¹⁷S. Kahl and A. M. Grishin, *J. Magn. Magn. Mater.* **278**, 244 (2004).
- ¹⁸B. Vertruyen, R. Cloots, J. S. Abell, T. J. Jackson, R. C. da Silva, E. Popova, and N. Keller, *Phys. Rev. B* **78**, 094429 (2008).
- ¹⁹M. Deb, E. Popova, A. Fouchet, and N. Keller, *J. Phys. D: Appl. Phys.* **45**, 455001 (2012).
- ²⁰M.-Y. Chern, F.-Y. Lo, D.-R. Liu, K. Yang, and J.-S. Liaw, *Jpn. J. Appl. Phys.* **38**, 6687 (1999).
- ²¹J. Hamrle, S. Blomeier, O. Gaier, B. Hillebrands, H. Schneider, G. Jakob, K. Postava, and C. Felser, *J. Phys. D: Appl. Phys.* **40**, 1563 (2007).
- ²²O. Gaier, J. Hamrle, S. J. Hermsdoerfer, H. Schultheiß, B. Hillebrands, Y. Sakuraba, M. Oogane, and Y. Ando, *J. Appl. Phys.* **103**, 103910 (2008).
- ²³J. M. Caicedo, S. K. Arora, R. Ramos, I. V. Shvets, J. Fontcuberta, and G. Herranz, *New J. Phys.* **12**, 103023 (2010).
- ²⁴J. M. Caicedo, M. C. Dekker, K. Dörr, J. Fontcuberta, and G. Herranz, *Phys. Rev. B* **82**, 140410 (2010).
- ²⁵D. Hrabovský, J. M. Caicedo, G. Herranz, I. C. Infante, F. Sánchez, and J. Fontcuberta, *Phys. Rev. B* **79**, 052401 (2009).
- ²⁶Q. M. Zhong, A. S. Arrott, B. Heinrich, and Z. Celinski, *J. Magn. Magn. Mater.* **104–107**, 1837 (1992).
- ²⁷S. Wittekoek, T. J. A. Popma, J. M. Robertson, and P. F. Bongers, *Phys. Rev. B* **12**, 2777 (1975).
- ²⁸G. B. Scott, D. E. Lacklison, H. I. Ralph, and J. L. Page, *Phys. Rev. B* **12**, 2562 (1975).
- ²⁹A. Aharoni, *Introduction to the Theory of Ferromagnetism* (Oxford University Press, Oxford, 1996).
- ³⁰N. Adachi, T. Okuda, V. P. Denysenkov, A. Jalali-Roudsar, and A. M. Grishin, *J. Magn. Magn. Mater.* **242–245**, 775 (2002).